DETERMINATION OF THE PRESSURE LOSS COEFFICIENT AT CONTROL-ROD GUIDE TUBE FLOW-HOLE FOR A PWR NUCLEAR FUEL ASSEMBLY BY USING CFD AND BERNOULLI SOLUTIONS

Dong-Yuan Sheng
Westinghouse Electric Sweden AB
72163, Västerås, Sweden
shengd@westinghouse.com

Marcus Seidl
E.ON Kernkraft GmbH
Tresckowstrasse 5, 30457 Hannover, Germany
marcus.seidl@eon.com

ABSTRACT

For accurate prediction of the margins to boiling inside the guide tube of a PWR fuel assembly the bypass mass flow and the guide tube heat source has to be determined. Historically due to a lack of numerical solution methods a conservative approach based on one-dimensional fluid analysis (e.g. Bernoulli principle, sudden contraction and expansion pressure loss) has been used. In reality the fluid moves in a complicated, three-dimensional way in the vicinity of the flow-hole: there is a sharp flow area change from fuel channel through the flow-hole into the guide tube together with two sharp 90 degree bends. In this study, a three-dimensional CFD model with full channel length has been developed to have a numerical determination of the flow-hole pressure loss coefficient. The ISO 5167 standard small sharp-edged cylindrical orifice was selected to validate the CFD model. The calculated values for the pressure loss coefficients (K_{in}) are in good agreement with the ISO standard. The developed model has been applied to calculate the pressure loss under different process parameters, such as: 1) Control rod position – to study the effect of control rod position on the mass flow in the guide tube; 2) Space grid – to study the guide tube mass flow influence on the effect of the pressure drop in the fuel channel; 3) Mass flow -- to study the relation between K_{in} and channel flow Reynolds number.

KEYWORDS
PWR, CFD, pressure loss coefficient, bypass, flow-hole

1. INTRODUCTION

In the design and safety analysis of a PWR, it is important to accurately predict the margins to boiling inside guide tubes (GT) under normal and abnormal operating conditions in order to exclude the possibility of stress corrosion cracking on inserted control rod fingers. The coolant mass flow from the fuel channel (FC) to the GT through the GT flow-hole together with the GT heat source are the main parameters to determine the margin to boiling. The pressure loss in a fuel assembly is an important parameter for this analysis because it controls the flow redistribution between FC and GT. To evaluate the mass flow through the flow-hole, measuring of the pressure loss would be the most commonly used approach. However the full scale real geometry measurement is difficult to set up due to the complex construction details. In these traditional designs, the few available conservative experimental correlations from the open literature or handbook for the maximum pressure loss coefficient at the GT inlet flow-holes were used. [1-2]

The traditional, conservative approach is based on one-dimensional (1D) fluid analysis (e.g. Bernoulli principle, sudden contraction and expansion pressure loss) to evaluate the pressure loss coefficient at GT inlet flow-holes. In reality the fluid moves in a complicated, three-dimensional (3D) way in the vicinity of the flow-hole: there is a sharp flow area change from fuel channel through the flow-hole into the guide tube (GT) together with two sharp 90 degree bends. This motivates our analysis to re-evaluate the value derived from the 1D method with modern computational tools.

Pressure loss coefficients of the cross flow between flow channels of nuclear fuel bundles have been studied by using theoretical and experimental analyses [3,4]. Computational fluid dynamics (CFD) offers a three-dimensional method for prediction of the pressure loss through flow-holes and has been widely used in recent years to model pressure loss through standard orifices [5-10]. Their results showed a good agreement between experimental data and CFD prediction viz. velocity/pressure profiles and discharge coefficients. The published results showed that the difference between simulated discharge coefficient C_D and values expected from the ISO 5167:2003 standard is lower than 5%. The reliability of predicting pressure loss coefficients with CFD methods in the above studies means that they potentially can be used as an alternative tool to determine best-estimate GT flow hole pressure loss coefficients instead of conducting time consuming experiments with a full length fuel assembly inside a flow channel test rig.

The objective of this study is to develop a 3D CFD model to get a numerical determination of the flow-hole pressure loss coefficient (K_{in}) at the guide tube for a PWR fuel assembly. The CFD model is validated with ISO 5167 – measurements of fluid flow by means of pressure differential devices inserted into circular-cross section conduits [11]. The developed model has been applied to calculate K_{in} at a GT inlet flow-hole under different process parameters, such as: 1) Control rod position – to study the effect of control rod position with regard to the mass flow in the guide tube; 2) Space grid – to study the guide tube mass flow influencing the effect of pressure drop in the fuel channel; 3) Mass flow -- to study the relation between K_{in} and channel Reynolds number. The numerical predicted pressure loss coefficients can be used as input for analysis the flow redistribution in the FC and GT based on Bernoulli's principle.

2. 1D MODEL AND 3D CFD MODEL

2.1. 1D model-- Bernoulli principle

The Bernoulli equation from flow hole inlet position to exit at guide tube top is written as (Figure 1):

$$\frac{1}{2}\rho_1 v_1^2 \quad + p_1 + \rho_1 g z_1 = \frac{1}{2}\rho_2 v_2^2 \quad + p_2 + \rho_2 g z_2 + \Delta p_f + \Delta p_h \qquad (1)$$

Where Δp_f is the pressure loss due to the friction on the inner GT channel surface and on the control rod surface, Δp_h is the pressure loss through the GT inlet flow-hole.

The mass balance equation gives:

$$F_1 \rho_1 v_1 = F_2 \rho_2 v_2 \qquad (2)$$

Combining eq. (1) and (2) yields a relationship for the exit velocity:

$$v_2 = \sqrt{\frac{2\Delta p - 2(\rho_2\, z_2\, g - \rho_1\, z_1\, g)}{\left(K_{in} - 1\right)\rho_1 \left(\frac{F_2\, \rho_2}{F_1\, \rho_1}\right)^2 + \rho_2 + \lambda\left(z_2 - z_1\right)\rho_2 / d_h}} \qquad (3)$$

The total pressure loss from guide tube flow-hole, along the control rod until the outlet is calculated as:

$$\Delta p_f + \Delta p_h = \lambda \frac{(z_2 - z_1)}{d_h} \frac{\rho_2}{2} v_2^2 \quad + K_{in} \frac{\rho_1}{2} v_1^2 \tag{4}$$

It can be found that K_{in} in Equation 3 and 4 is a key coefficient to determine the total pressure drop and mass flow in the GT channel.

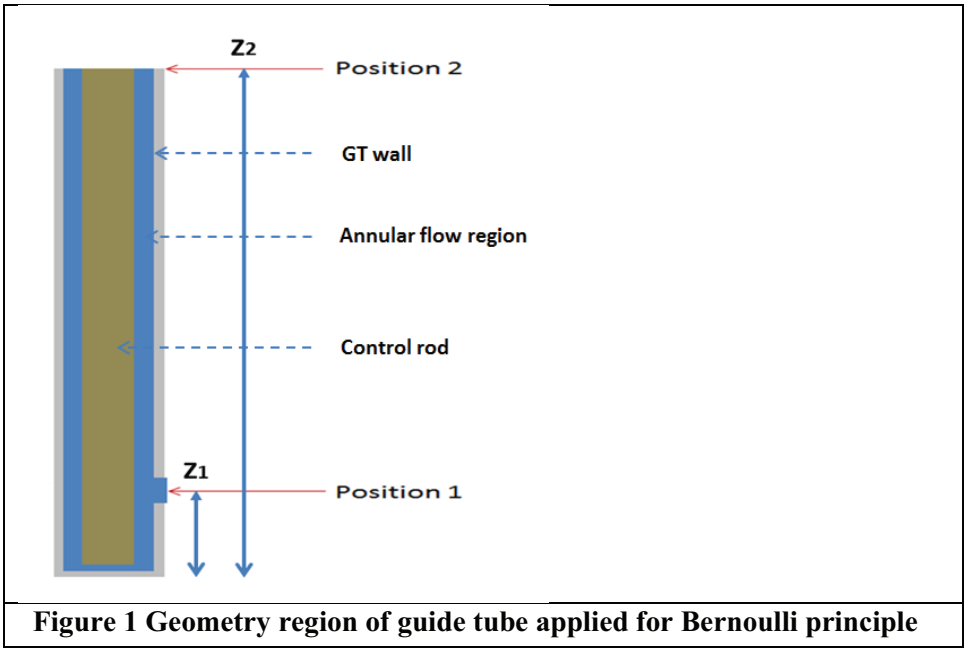

Figure 1 Geometry region of guide tube applied for Bernoulli principle

2.2. 3D CFD model

2.2.1. Governing equations

The calculation of single-phase incompressible flow is accomplished by solving the mass and momentum conservation equations given as:

Continuity equation:

$$\frac{\partial(\rho)}{\partial t} + \frac{\partial}{\partial x_i}(\rho u_i) = 0 \tag{5}$$

Momentum equation:

$$\frac{\partial}{\partial t}(\rho u_i) + \frac{\partial}{\partial x_j}(\rho u_i u_j) = -\frac{\partial P}{\partial x_i} + \frac{\partial \tau_{ij}}{\partial x_j} + S_{F_i} \tag{6}$$

where x_i are the Cartesian coordinates; u_i are the corresponding average velocity components; t is the time; ρ is density; P is pressure; τ_{ij} are stress tensor components; S_{Fi} are the source terms for momentum equations.

The success of numerical prediction methods depends to a great extent on the performance of the turbulence model used. From the literature review in section one, it can be seen that the Realizable k-ε and SST k-ω model are the most commonly used turbulence model in the simulation of the flow through small holes. The Realizable k-ε model is considered to be valid for fully developed turbulent and non-separated flow [12]. SST k-ω turbulence model is considered to be suitable for dealing with partially separated or swirl flow [13]. In this study, the two turbulence models are selected and compared with the ISO 5167 standard.

Realizable k-ε model:

$$\frac{\partial}{\partial t}(\rho k)+\frac{\partial}{\partial x_j}(\rho k u_j)=\frac{\partial}{\partial x_j}\left[\left(\mu+\frac{\mu_t}{\sigma_k}\right)\frac{\partial k}{\partial x_j}\right]+G_k+G_b-\rho\varepsilon-Y_M+S_k \quad (7)$$

$$\frac{\partial}{\partial t}(\rho \varepsilon)+\frac{\partial}{\partial x_j}(\rho \varepsilon u_j)=\frac{\partial}{\partial x_j}\left[\left(\mu+\frac{\mu_t}{\sigma_\varepsilon}\right)\frac{\partial \varepsilon}{\partial x_j}\right]+\rho C_1 S\varepsilon-\rho C_2\frac{\varepsilon^2}{k+\sqrt{v\varepsilon}}+C_{1\varepsilon}\frac{\varepsilon}{k}C_3 G_b+S_\varepsilon \quad (8)$$

Where k is turbulent kinetic energy; ε is turbulent energy dissipation rate; μ is molecular viscosity; μ_t is turbulent viscosity; G_k represents the generation of turbulent kinetic energy due to the mean velocity; Y_M represents the contribution of the fluctuating dilatation in compressible turbulence to the overall dissipation rate; υ is kinematic viscosity; σ_k and σ_ε are the turbulent Prandtl numbers for k and ε respectively.

SST k-ω turbulence model:

$$\frac{\partial}{\partial t}(\rho k)+\frac{\partial}{\partial x_j}(\rho k u_j)=\frac{\partial}{\partial x_j}\left(\left(\mu+\frac{\mu_t}{\sigma_k}\right)\frac{\partial k}{\partial x_j}\right)+G_k-Y_k \quad (9)$$

$$\frac{\partial}{\partial t}(\rho \omega)+\frac{\partial}{\partial x_j}(\rho \omega u_j)=\frac{\partial}{\partial x_j}\left[\left(\mu+\frac{\mu_t}{\sigma_\omega}\right)\frac{\partial \omega}{\partial x_j}\right]+G_\varpi-Y_\omega \quad (10)$$

where ω is turbulent energy dissipation rate; G_k represents the generation of turbulent kinetic energy due to mean velocity gradients; G_ω represents the generation of ω; σ_ω is the turbulent Prandtl numbers for ω; Y_k and Y_ω represent the dissipation of k and ω due to turbulence.

Though some other turbulence models (Reynolds stress model, RSM and Large eddy simulation, LES) have been reported to be superior to others in some flow scenarios, there is no universal turbulence model that is best for all flow conditions. Considering the complexity of the geometry, the total number of elements is expected to be large and turbulence models that require fine meshes were ruled out in the first step of this study.

2.2.2. Computational details

The CFD calculation domain is built for four fuel sub-channels (2x2), and one GT channel. The geometry is shown in Figure 2. The simulations are performed with the commercial CFD code -- Star-CCM+ v.9.02. A three dimension, steady state and segregated solver was used. The second-order upwind scheme is used to calculate the convective flux. The discretized equations were solved in a segregated manner with the semi-implicit method for pressure-linked equations (SIMPLE) algorithm [14]. The solutions were considered to be converged when the sum of the normalized residuals for all the cells became less than 10^{-4} for the variables:

$$R^{\emptyset}=\frac{\sum_{cellsP}\left|\sum_{nb} a_{nb}\emptyset_{nb}+b-a_p\emptyset_p\right|}{\sum_{cellsP}\left|a_p\emptyset_P\right|} \quad (12)$$

Where ϕ_p and ϕ_{nb} are the variable of the present and neighboring cells, respectively, a_p is the coefficient of the present cell, and a_{nb} are the coefficients for the neighboring cells, b is the contributions of the constant part of the source term and boundary conditions.

2.2.3. Mesh and boundary conditions

The computational domains were discretized with an unstructured polyhedral mesh with a prismatic elements layer in the region near the walls in order to adequately capture the flow gradients in such areas. Meshes are refined in the flow-hole region. Mesh extrusion is used for inlet and outlet parts in order to simulate the full flow channel. A mesh independency study was performed to find a mesh that was sufficiently fine to provide an accurate solution. The geometries are imported from a CAD model created by Pro/Engineer. In order to create a high quality CFD mesh the de-featuring technique was used to remove those small features in the CAD model (such as smaller fillets, smaller faces/edges, small holes), which have little effect on the result. The mixing vanes, grid strap, spring and dimple in fuel channel are simplified by using the porous media model. The computational domain is shown in Figure 2 and the CFD mesh is shown in Figure 3. The rod pitch is 14.3 mm. The outer and inner diameter of GT are 13.8 mm and 12.4 mm. Bypass flow-hole diameter is 2.6mm. 8 porous media regions were defined to simulate space grids. Grid span length is 534 mm. The isotropic inertial (quadratic) and viscous (linear) resistance are defined as source terms in the momentum equation. The coefficients for inertial and viscous resistance are 6300 kg/m4 and 6000 kg/m3-s. The polyhedral mesher, with the embedded prism layer mesher, was used to build the volume mesh in the region close the bypass hole. The extruder mesh was used to generate the volume mesh in the channel in order to produce the orthogonal extruded cells (Figure 3). Mesh independency studies have been performed with the focus on the bypass mass flow. Mesh independence occurred at approximately 6 million volume meshes. The surface average y+ is around 60 and maximum y+ is around 110.

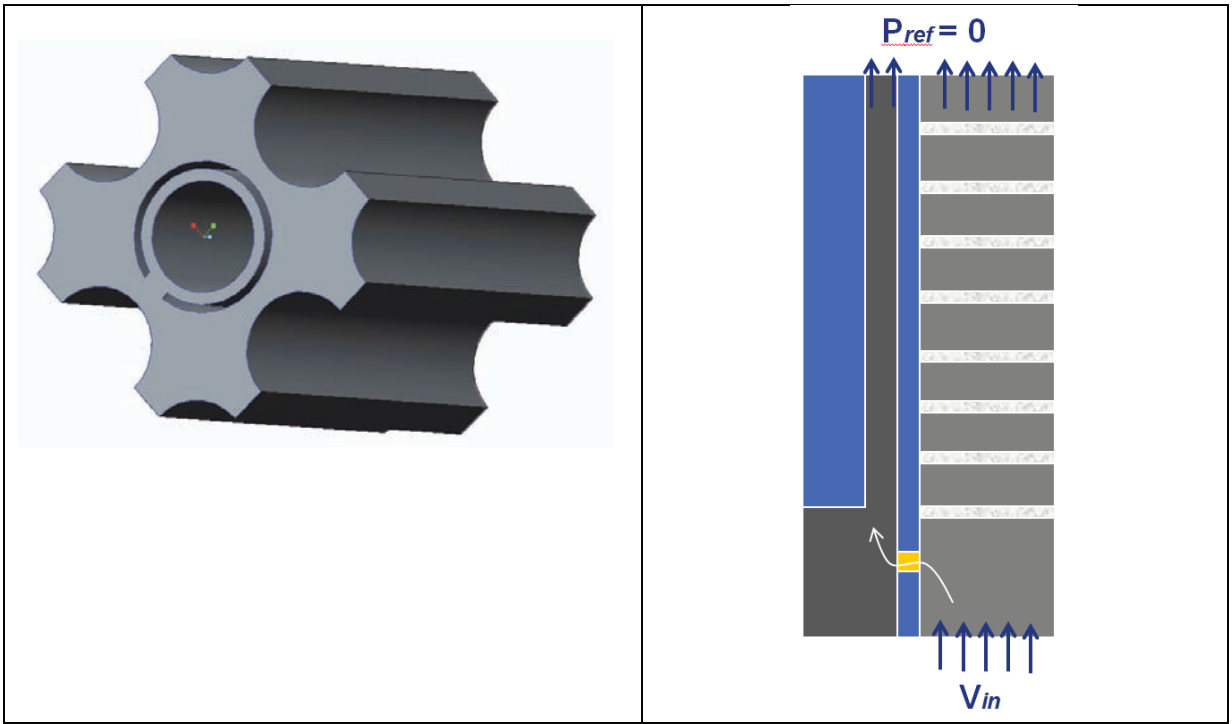

a) flow channel	b) flow boundary

Figure 2 Geometry of flow calculation domain

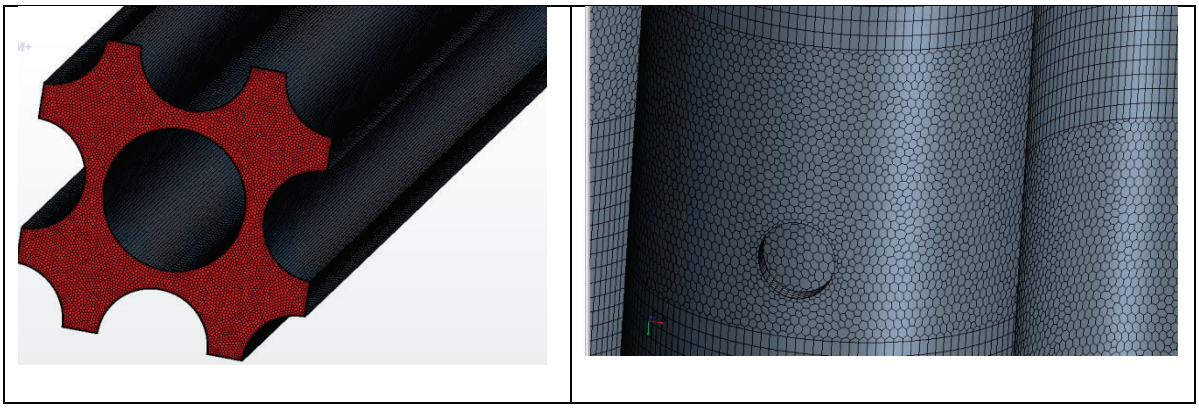

Figure 3 CFD computational meshes

In all simulations, a velocity inlet boundary condition is used at the inlet of the fuel channel (V_{in} in Figure 2b). A wall function is applied to bridge the viscous sub-layer and provide near-wall boundary conditions for the mean flow and the turbulence transport equations. The wall conditions are connected by means of empirical formulae to the first grid node close to the solid surfaces [15]. The input parameters for simulation are listed in Table 1. Pressure outlet boundary conditions (P_{ref}=0) are set up at the top plane of both fuel channel and GT channel. Symmetric boundary conditions are applied at the rod gap.

Table 1 Process parameters and physical properties

Parameter	Dimension	Value
Inlet velocity	m/s	1,2,3,4,**5**,6
Density	kg/m^3	746.2
Viscosity	Pa·s	$9.24 * 10^{-5}$
Pressure	Bar	155
Inlet Temperature	°C	290
GT inner diameter	Mm	12.4
CR outer diameter	Mm	13.8

3. VALIDATION OF CFD MODELS

The ISO standard 5167 is selected to validate the CFD model. The principle of this ISO standard is based on the installation of an orifice plate into a pipeline in which a fluid is flowing. This standard gives the detailed geometry design, installation and operation conditions. The presence of the orifice plate causes a static pressure difference between the upstream and downstream sides of the plate. The mass flowrate, Q_m, can be determined using the following equation

$$Q_m = \frac{C_D}{\sqrt{1-\beta^4}} \varepsilon_l \frac{\pi}{4} d^2 \sqrt{2\Delta P_d \rho} \qquad (13)$$

Where C_D is discharge coefficient, ΔP_d is differential pressure, d is orifice hole diameter, D is pipe diameter, β is diameter ratio (d/D), ε_l is expansion factor, for liquids it is constant one.

The discharge coefficient C_D relates the actual flow-rate to the theoretical flow-rate through a device. It is related with the turbulence of the flow and the restriction the device makes to the flow. To calculate the discharge coefficient from empirical data, ISO 5167 gives the large Reader-Harris/Gallagher formula [16]. For each orifice plate, at least one upstream pressure and one downstream pressure taps are installed in one or other of standard location, i.e. as D and D/2, flange or corner tappings. The corner tapping results are used to validate the CFD results.

The pressure loss ΔP for the orifice plates described in ISO5167 is approximately related to the differential pressure ΔP_d by Equation (14),

$$\Delta P = \frac{\sqrt{1-\beta^4\left(1-{C_D}^2\right)}-C_D\beta^2}{\sqrt{1-\beta^4\left(1-{C_D}^2\right)}+C_D\beta^2}\Delta P_d \qquad (14)$$

The pressure loss ΔP is the permanent pressure loss through the orifice plate and the pressure recovery downstream from orifice is excluded from the differential pressure ΔP_d. Figure 4 shows the pressure and velocity contour in the center cross section based on the CFD simulation.

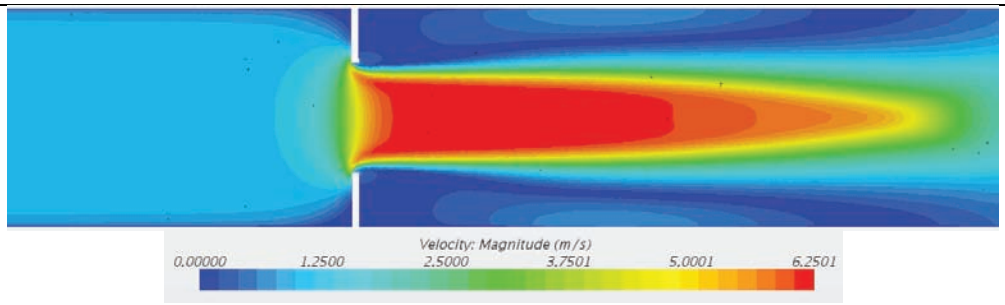

a) Velocity contour

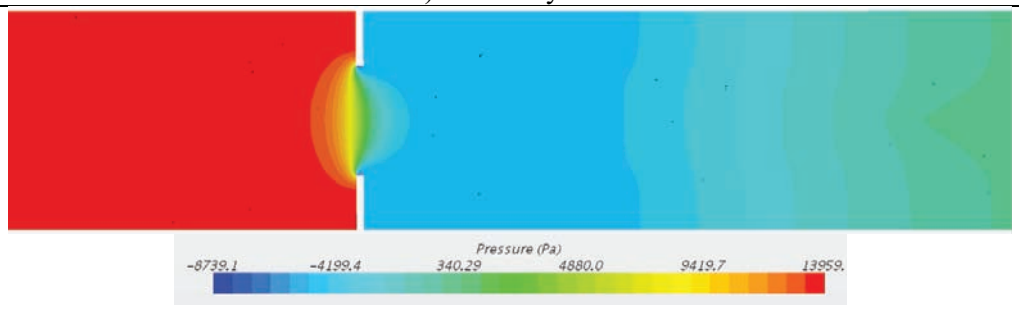

b) Pressure contour

Figure 4 Velocity and pressure contour in the middle cross section

While flowing through the orifice plate the fluid undergoes a flow contraction that is followed by a flow expansion. During flow contraction the flow velocity increases and the static pressure decreases (Bernoulli). Here, the potential energy is transformed into kinetic energy without significant energy losses. During flow expansion after passing through the hole, the flow velocity decreases and the static pressure increases (Figure 4). Fluid flow in the direction of increasing pressure results in a significant pressure loss. Figure 5 shows the pressure loss through the orifice plate along the center streamline. The differential pressure ΔP at the orifice plate is 19000 KPa and the pressure loss ΔP_d (permanent pressure loss) is 14000 KPa. The comparison between CFD predictions and ISO standard is shown in Table 2. The Discharge coefficient can be used to directly compare the results and the difference is smaller than 3.1%.

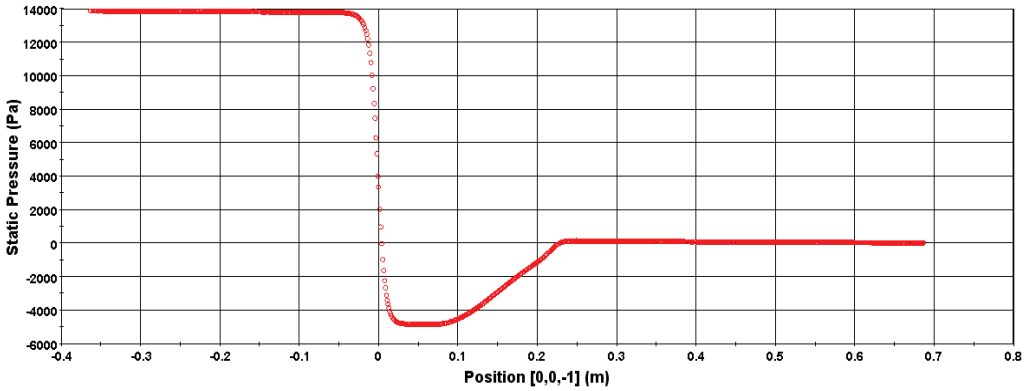

Figure 5 Predicted pressure through orifice plate along center streamline

Table 2 Comparison of CFD and ISO 5167

	Discharge Coefficient (C_D)	Difference (C_D)	Pressure loss (ΔP)	Difference (ΔP)
ISO 5167	0.608		14000	
CFD	0.627	3.1%	14550	3.9%

The turbulence model study was completed by using two different turbulence models described previously, namely Realizable k-ε and k-ω SST. Figure 6 shows the pressure loss through the orifice plate along the center streamline with the two different turbulent models. The Realizable k-ε and k-ω SST models predict nearly the same differential pressure ΔP at the orifice plate. A slight difference is observed at the downstream of orifice plate. The Realizable k-ε model is selected for the calculations shown in the next section.

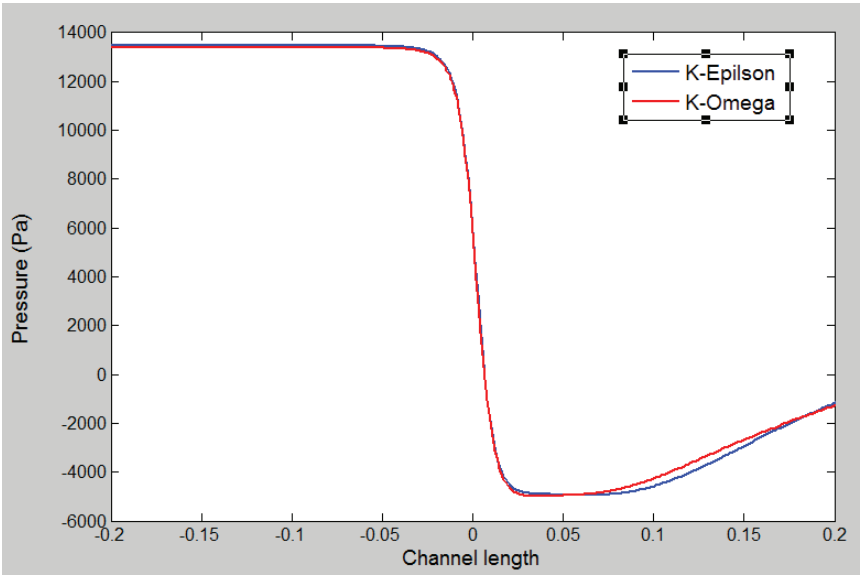

Figure 6 Pressure losses through the orifice along streamline with the different turbulent models

4. RESULTS AND DISCUSSION

The CFD model was applied in predicting the pressure loss for a PWR fuel assembly using the same procedure as in the previous sub-section. To study the pressure loss through the GT flow-hole, the CR position, the FC mass flow and the spacer grids were used as geometry structure and process parameters. Based on the CFD results, the effects of different geometries and process parameters on the pressure loss coefficients of the GT flow-hole was predicted.

4.1 CR position

In the following two limiting cases for the control rod position are analyzed. In the first case the control rod is fully inserted and extends beyond the flow hole to the bottom of the GT. In the second case the control rod tip is standing just above the flow-hole position. The first case is limiting with regard to the maximum heat source within the GT. The second case is limiting with regard to the minimum mass flow within the GT because in this case the pressure loss through the flow whole will be maximal. Figure 7 shows the velocity contour at two different cross sections for both cases: control rod close to channel bottom, and close to channel outlet. The inlet velocities are set to 5 m/s at the bottom plane of the fuel channel and it is uniformly distributed at this plane. The blue color in the GT channel means a low velocity and stagnation region below the flow hole. To the region close to the outlet, it shows a fully developed channel flow pattern in the fuel channel. The increase of velocity in the GT means the bypass flows through the flow hole.

Figure 8 shows the pressure drop along streamlines in the different cases. Two typical streamlines are selected: one is in the center of fuel channel and the other is in the center of flow hole. The inlet pressure drop (at Y= 0.0 position) is calculated from the exported CFD data. The flow-hole's pressure drop is marked by the red arrow in the figure.

The pressure loss at inlet flow-hole can be written as Equation 15:

$$\Delta P = K_{in} * \frac{1}{2}\rho v^2 \qquad (15)$$

The calculation parameters of the pressure loss coefficient K_{in} are listed in Table 3. The velocities of the inlet hole (v) is calculated by the using the GT outlet velocities.

The results of the two CFD simulation cases show that:

1) The inlet velocities through the flow hole are quite similar for the two cases.
2) The pressure drops through the flow hole are similar. The pressure curves show same tendency in the GT.
3) The calculated pressure loss coefficients is 2.8 (CR fully inserted) and 2.9 (CR 1 cm above flow hole). The inlet pressure loss coefficients through the flow hole are not sensitive to CR positions in the GT which indicates that the movement of CR in the guide tube has a minor effect to the inlet pressure loss. Traditionally both cases were analyzed to determine the minimum mass flow through the GT. In most of these analyses the second case turned out to be the most limiting one because by using standard, conservative formulas for the pressure loss through the expansion of the fluid from the small flow-hole area to the full GT area the minimum mass flow occurred. CFD analysis indicates that a fully inserted control rod is the limiting case for the margin to boiling safety analysis because it has the maximum possible heat source.

Table 3 Calculated pressure loss coefficient by using CFD results

Parameter	Annular Flow	CR 1cm above hole
GT outlet velocity (m/s)	0.77	0.76
Hole inlet velocity (m/s)	5.639	5.575
Density (kg/m^3)	746.2	746.2
Pressure Loss (KPa)	33	33.5
Pressure Loss Coefficient	2.8	2.9

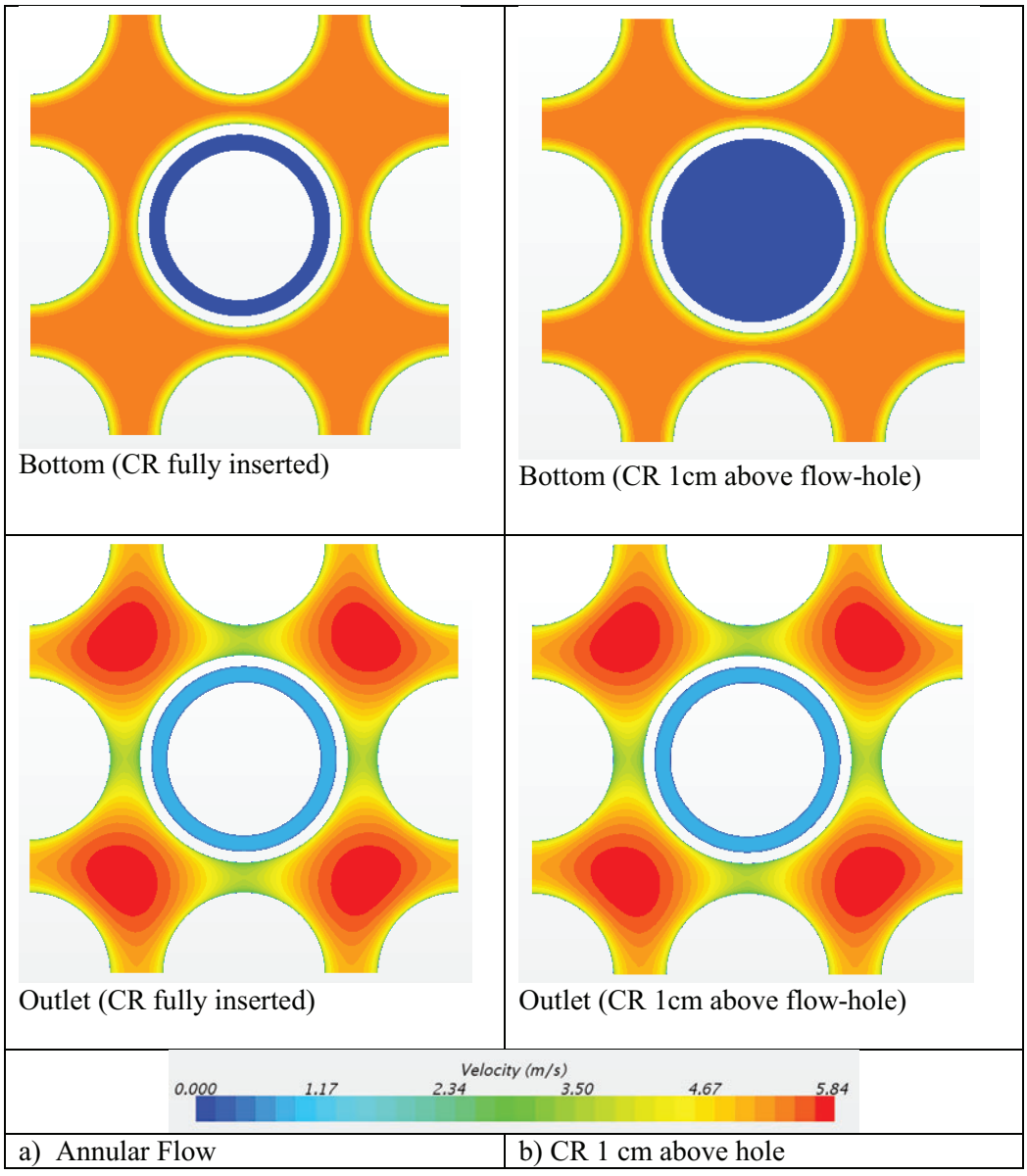

Figure 7 Velocity contours on two different cross sections in channel

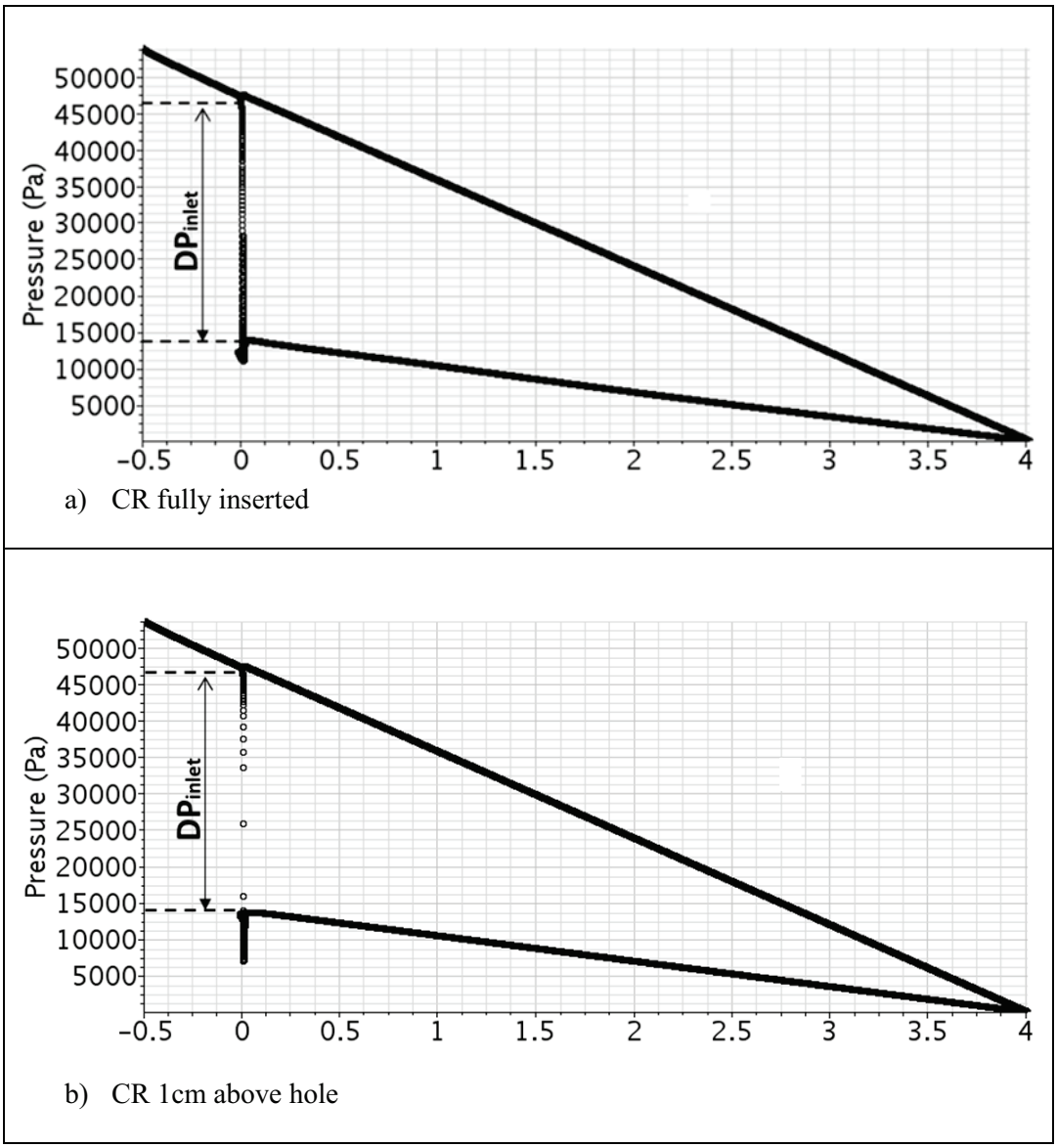

Figure 8 Pressure drop along streamlines

4.2 Space grid

The CFD simulation region consists of two parallel channels (FC and GT) with different geometrical configuration and hydraulic diameter. There is a pressure equalization process for FC and GT channels due to the bypass flow through GT inlet hole. The spacer grids and fuel rod friction determine the pressure drop in the fuel channel, while the GT inlet hole and the CR friction determine the pressure drop in the GT channel.

As shown in Figure 2b, there are eight spacer grids above the GT inlet flow-hole in this design. The spacer grids have many small components with thickness of 1-2mm. The geometric complexity requires the adoption of a finer mesh. To reduce computational time and effort, the porous media approach for the spacer grids is applied in this study. Porous media are modeled by the addition of a momentum source term to the standard fluid flow equations. The source term is composed of two parts: a viscous term and

an inertial loss term. The spacer grids are simplified solid material with uniformly dispersed in the flow domain. The porosity and flow resistance replicate the volume-average characteristics of their real geometrical domain.

Figure 9 Calculated pressure drop in the fuel channel (with 8 spacer grids) and GT channel

Figure 9 shows the CFD calculated pressure drop in the fuel and the GT channel. The pressure drop along the fuel rods is considered to be due to friction and the pressure drop in the spacers is calculated by using the porous medium model. The total pressure drop increased in the fuel channel due to the spacers compared with the case without spacers (Figure 7). The higher pressure drop in the fuel channel leads to an increased mass flow through the GT inlet hole. The calculated pressure loss coefficients is 2.3 which is 0.5 lower than the case without spacer grids (Kin=2.8). One explanation to the lower Kin with spacer grid is that the first spacer grid is about 7 cm above the GT inlet hole. The closed distance between spacer grid and GT inlet hole will change the local flow pattern, flow angle to GT inlet and turbulence strength near the GT inlet hole.

4.3 Mass Flow

Parametric studies were done which characterize the pressure loss coefficient K_{in} as the Reynolds number changes. Six different cases were set up with the fuel channel inlet velocities as 1,2,3,4,5,6 m/s. The mass flow through the GT inlet hole is increased when increasing the fuel channel inlet velocity. The results show that the pressure loss coefficient remains essentially constant across the range of Reynold number between $1x10^5$ and $7x10^5$.

5 CONCLUSIONS

A 3D CFD model to predict the flow-hole pressure loss coefficient (K_{in}) at the guide tube for a PWR fuel assembly has been developed in this study. The validity of the developed CFD model was evaluated with the help of the ISO 5167:2003 standard. A comparison of the Realizable k-ε and the SST k-ω turbulence models have been done. The two turbulence models predict nearly the same differential pressure ΔP at the orifice plate in the ISO reference. A slight difference is observed downstream of the orifice plate. The discharge coefficient is smaller than 3.1% by comparing CFD results and the ISO standard result.

The results of the CFD simulations on different control rod positions show that the GT hole inlet mass flow and pressure drops are quite similar. The calculated pressure loss coefficients is 2.8 (CR fully inserted) and 2.9 (CR 1 cm above flow hole). The inlet pressure loss coefficients through the flow hole are not sensitive to CR position which indicates that the movement of the CR in the guide tube has a minor effect to the inlet pressure loss. Traditionally, in most of these analyses the second case turned out

to be the most limiting one because, by using standard, conservative formulas for the pressure loss through the expansion of the fluid from the small flow-hole area to the full GT area, the minimum mass flow occurred. This analysis shows that a fully inserted control rod (the first case) is the limiting case for the margin to boiling safety analysis because it has the maximum possible heat source.

The total fuel assembly pressure drop is increased due to the flow resistance of the spacer grids. The higher pressure drop in the fuel channel leads to an increased mass flow through the GT inlet hole. The calculated pressure loss coefficient is 2.3 which is 0.5 lower than the case without spacer grids. Six different cases (with space grids) were done with channel inlet velocities as 1,2,3,4,5,6 m/s. The results show that pressure loss coefficient remains essentially constant across the range of Reynold number between $1x10^5$ and $7x10^5$.

REFERENCES

1. I. E. Idelchik: *Handbook of Hydraulic Resistance*, 3rd Edition, Boca Raton, CRC press (1994)
2. J. Stichlmair: "Druckverlust bei der Durchströmung von Lochplatten", *VDI-Wärmeatlas* (2006)
3. J. Weisman, "Cross flow resistance in rod bundle cores", *Nuclear Technology*, **15**(9),pp. 465-469 (1972)
4. C. H. Shin, T. H. Chun, D. S. Oh and W. K. In, "Evaluation of loss coefficient for an end plug with side holes in dual-cooled annular nuclear fuel", *Journal of Mechanical Science and Technology*, **26**(10), pp.3119-3124 (2012)
5. M. K Roul and S. K. Dash, "Numerical modeling of pressure drop due to single phase flow of water and two-phase flow of air-water mixtures through thick orifices", *Int. J. of Engineering trends and technology*, **3** (4), pp. 544-551 (2012)
6. Erdal and H. I. Andersson, "Numerical aspects of flow computation through orifices", *Flow Meas. Instrum.*, **8**(1), pp.1-11(1997)
7. J. Q. Chen, B. Wang, B. Wu and Q. D. Chu,"CFD simulation of flow filed in standard orifice plate flow meter", *J. of Experiments in Fluid Mechanics*, **22**(2), pp. 51-55(2008)
8. F. H. J. Imada, F. Saltara and J. L. Balino, "Numerical determination of discharge coefficients of orifice plates and nozzles", *Proceedings of 22nd International Congress of Mechanical Engineering*, Riberirao Preto, Brazil, pp. 1755-1760 (2013)
9. M. S. Shah, J. B. Joshi, A. S. Kalsi, C. S. R.Prasad and D. S. Shukla, "Analysis of flow through an orifice meter: CFD simulation", *Chemical Engineering Science*, **71**, pp. 300-309 (2012)
10. V.V. R. Kaushik, S. Ghosh, G. Das and P. K. Das, "CFD simulation of core annular flow through sudden contraction and expansion", *J. of Petroleum Science and Engineering*, **86-87**, pp.153-164 (2012)
11. ISO 5167, *Measurement of fluid flow by means of pressure differential devices inserted in circular-cross section conduits running full*, Int. Stand Org. (2003)
12. T.H. Shih, W. W. Liou, A. Shabbir, Z. Yang and J. Zhu, "A new k-ε eddy viscosity model for high Reynolds number turbulence flows- model development and validation", *Computers Fluid,* **24**(3), pp. 227-238 (1995)
13. D. C. Wilcox, "Formulation of the k-omega turbulence model revisited", *AIAA journal*, **46**(11), pp. 2823-2838 (2008)
14. S. V. Patankar and D. B. Spalding, "A calculation procedure for heat, mass and momentum in three-dimensional parabolic flows", *International Journal of Heat and Mass Transfer*, pp.15 (1972)
15. B. E. Launder and D. B. Spalding, "The numerical computation of turbulent flows", *Computatioinal Methods in Applied Mechanics and Engineering,* **3**(3), pp. 269-289 (1974)
16. M. J. Reader-Harris and J. A. Sattary, "The orifice plate discharge coefficient equation – the equation for ISO 5167-1", *Proceedings of 14th North Sea Flow Measurement Workshop*, Scotland, pp. 24 (1996)